Original Article

The association of peak systolic velocity in the carotid artery with coronary heart disease: A study based on portable ultrasound

Carola S König[1] , **Mark Atherton[1]** , **Marco Cavazzuti[1,2]** ,
Corinna Gomm[3] and Sudarshan Ramachandran[1,3,4]

Abstract
Cardiovascular disease (CVD) is the highest cause of death globally with more people dying annually from it than from any other cause. CVD is associated with modifiable risk factors (dyslipidaemia, hypertension and diabetes) and treating each of these factors lowers the risk of CVD. It is impossible to estimate the benefit of risk factor modification in the individual patient and extrapolating data from multiple trials is difficult. It would be useful to have a marker of risk that accurately estimates real time risk by measuring blood flow factors associated with the pathogenesis of atheroma. The aim of this preliminary study was to validate a low-cost measurement technique for obtaining blood flow velocity profiles and assess whether any of the measured and calculated factors, based on computational fluid dynamics (CFD) simulation, known to be associated with atheroma was associated with coronary heart disease (CHD), thus establishing its feasibility and acceptability as a clinical tool and suggesting areas for future research. Our study identified (i) that mean peak systolic (PS) velocity being associated with CHD; individuals without CHD: mean (SD) = 62.8 (16.1) cm/s, with CHD: mean (SD) = 53.6 (17.3) cm/s, $p = 0.042$; and (ii) that low-cost, portable ultrasound, which is routinely available in general practice, is a suitable assessment tool.

Introduction

Cardiovascular disease (CVD) accounted for nearly a quarter of deaths in the UK (152,465 of 597,206 deaths) in 2016.[1] Studies such as the Framingham Heart Studies and Munster Heart Study have established that CVD is associated with modifiable risk factors such as hyperlipidaemia, hypertension, diabetes, smoking in addition to age, male gender and a positive family history.[2] Importantly many intervention studies treating each of these modifiable risk factors have led to lowering of CVD.[3] These trials have formed the cornerstone of an evidence-based approach to CVD prevention and have resulted in various guidelines for each of the above-mentioned risk factors; i.e. NICE guidelines, Joint British Societies guidelines.[4,5]

Although this approach of treating risk factors would be expected to result in benefit, it is impossible to estimate benefit non-invasively whilst treating the patient. Further, as clustering of risk factors is often present many of the risk factors are simultaneously addressed in the same patient.[6,7] Evidence from randomised controlled trials (RCT) seldom investigates interaction of parallel treatment effects, which is common in

[1]Department of Mechanical and Aerospace Engineering, Brunel University London, England, UK
[2]Department of Engineering 'Enzo Ferrari', University of Modena, Italy
[3]Department of Clinical Biochemistry, University Hospitals Birmingham Foundation Trust, West Midlands, England, UK
[4]Department of Clinical Biochemistry, University Hospitals of North Midlands/Faculty of Health Sciences, Staffordshire University/Institute of Science and Technology, Keele University, Staffordshire, England, UK

Corresponding author:
Carola S König, Department of Mechanical and Aerospace Engineering, Brunel University London, Kingston Lane, Uxbridge, England, UB8 3PH, UK.
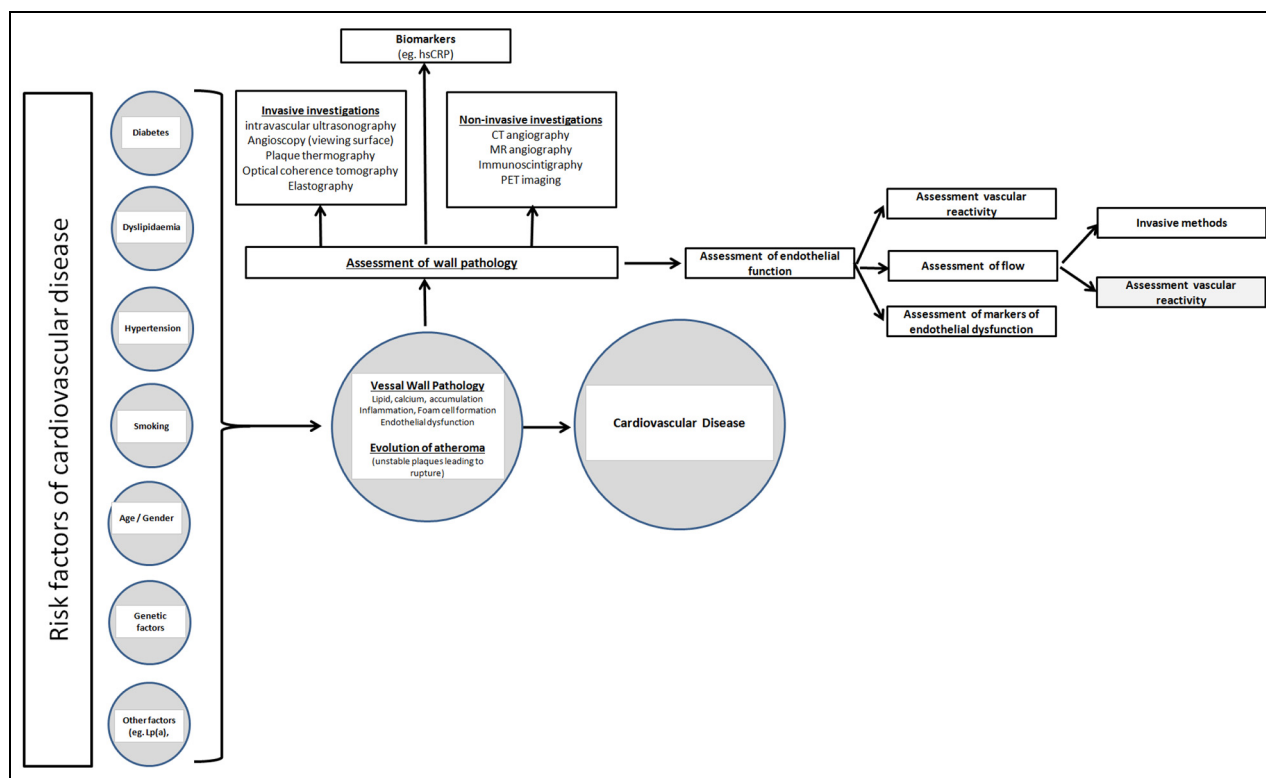Email: carola.koenig@brunel.ac.uk

Figure 1. A scheme of risk factors and the various options to assess real time atherogenesis together with possible mechanisms to investigate the state of the endothelium is presented.

clinical practice. Thus, benefits observed in individual RCTs may not accurately translate to such patients encountered in a routine out-patient setting.

Ideally a near-patient estimation of a non-invasive marker involved in the pathogenesis of CVD would be useful to determine therapeutic effectiveness.[8,9] Currently there is no routinely non-invasive method to directly study cumulative risk reduction when multifaceted risk reduction intervention is available in the NHS in the UK. Such assessment would be useful in a patient with diabetes where treatment is often targeted at improving glycaemic control, dyslipidaemia, hypertension, renal function etc. all of which have effects on cardiovascular risk.[7] A scheme of various options assessing real time atherogenesis is presented in Figure 1.

Vascular wall properties such as endothelial function, inflammation and smooth muscle proliferation are considered important in the pathogenesis of atherosclerosis.[8] Both, risk and protective factors of CVD may influence the integrity of the endothelium. Endothelial dysfunction is considered reversible by risk factor modification.[8–10] Thus, it is tempting to speculate that assessing the state of the endothelium could be beneficial in assessing the risk of the individual. Although it is the state of the coronary arteries that is of paramount interest in the development of coronary heart disease (CHD) it is seen that endothelial dysfunction represents a systemic disorder of the entire arterial

system. Figure 1 summarises the methods that could be used to assess the state of the endothelium.

Vascular flow patterns can be affected by characteristics of the arterial wall and result in such in endothelial dysfunction.[10] Thus, it is reasonable to assume that studying suitable parameters of blood flow in the arterial vasculature is possibly a method that could be utilised to estimate cumulative cardiovascular risk. Interestingly Halcox et al.[11] demonstrated that coronary endothelial dysfunction independently predicted acute cardiovascular events. Conventional atherosclerosis risk factors such as diabetes, dyslipidaemia, smoking and hypertension have been seen to alter endothelial cell function.[11,12]

It has been seen that endothelial function has been associated with vascular flow characteristics.[13] The pathogenesis of atherosclerosis is associated with both vessel wall injury and other factors, both systemic and local.[13] It is suggested that atherosclerosis is related to altered wall shear stress (WSS), particularly low WSS, due to a decrease in nitric oxide synthase production, vasodilation and cell repair.[14–17] Malek et al.[18] identified that WSS $> 1.5\,Pa$ induces endothelial quiescence and an atheroprotective gene expression profile, while values $< 0.4\,Pa$ were found at atherosclerosis-prone sites resulting in stimulating an atherogenic phenotype. Gijsen et al.[19] classed WSS between 0 and 1 Pa as 'low' while the range from 1 to 7 Pa was being classed as 'normal/high' as in cultured endothelium the range from 1.2
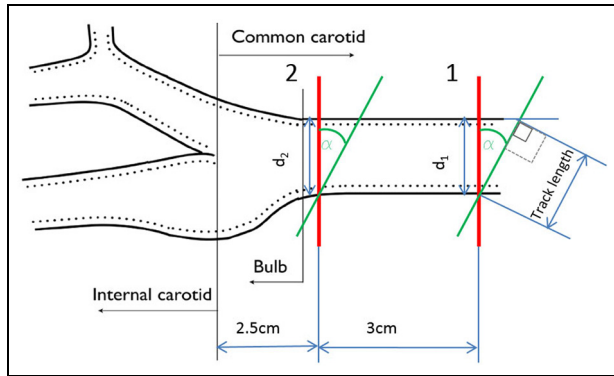
Figure 2. A diagrammatic view of the data collection site.

to 1.5 Pa was found to be most frequently atheroprotectively associated though a plaque stenosis could see values of 7 Pa and higher. A marker of overall vascular risk could possibly be obtained from Computational Fluid Dynamics (CFD) models derived from flow characteristics obtained in turn from non-invasive techniques. As the modelling is comprehensive (three-dimensional and if necessary time-dependent) it is able to provide complete predictive data for the derivation of local wall shear stress. As explained by Cunningham and Gotlieb[20] the shear stress has a possible direct association with atherosclerosis: by studying its variation and how it connects with the mechanism(s) of atherosclerosis it may provide estimates of both, risk estimate and benefit in a real world setting. For routine use, a non-invasive method as suggested by Chhabra[9] is ideal in an out-patient setting. An easily accessible blood vessel with flow characteristics suitable for the resolution, precision and accuracy of ultrasound (US) flow estimation such as the carotid artery is potentially an ideal start point. To explore the possibility of using US flow parameters to study atherogenesis we embarked on a study to derive a dataset necessary to enable computational risk flow data to be used clinically. We wished to study these parameters in different patient groups investigating the association between the derived values and estimated risk (comparison of patients with established coronary heart disease (CHD) and individuals not experiencing symptoms). In the event of an association we hoped to design prospective studies to establish whether any factors measured or derived by US could predict real time atheroma. The aim of this paper was to assess whether flow associated factors, measured or derived from non-invasive carotid US was associated with atheroma.

We would like to stress that whilst both, US Doppler velocimetry and echo particle image velocimetry have been applied in vitro and in vivo for similar applications, with the benefit of being capable to provide flow data at higher accuracy,[21–24] this study was conducted purposefully on routinely available portable US equipment to allow for uptake as a possible routine diagnostics tool.

Materials and methods

Patients

Patients (≥18 years of age) with established CHD but without known cerebrovascular disease (as carotid atheroma could have potentially distorted measurements) were identified from the Dyslipidaemia Clinics at University Hospitals Birmingham NHS Foundation Trust. All the above patients had an angiogram demonstrating significant atheroma, hence they were referred for secondary CVD prevention. None of the patients had presented with symptoms/signs of cerebrovascular disease. Sample size was determined *a priori* for a *t*-test on the difference between two independent means (two groups of equal size: mean WSS for healthy individuals vs those with established CHD) using GPower.[25] Mean and standard deviation of WSS at peak systole is expected to be 1.87 Pa and 0.41 Pa, respectively for healthy subjects, and 1.53 Pa and 0.40 Pa for subjects with established CHD[26]; thus, the effect size calculated by GPower is 0.84 Pa, whereas the smallest change in WSS detected was 0.34 Pa. The above data suggested a minimum sample of 26 subjects (Alpha = 0.05 and Power = 0.90) in each arm. We fixed 4 days of recruitment/US scanning having approached eligible patients with CHD in previous clinics whilst controls (≥ years of age) were recruited from health service professionals and patient relatives; this approach led to 27 patients with established CHD and 30 individuals without symptoms suggestive of CHD to be included. Exclusion criteria included individuals to provide written informed consent, those with a history of prior carotid surgery, carotid disease, superior vena cava obstruction or any other event or procedure that would affect the vascular anatomy, local blood flow or pressure (CG, a vascular ultrasonographer had final responsibility for making and documenting this decision) and cardiac arrhythmias, individuals unable to tolerate lying semi-prone for 30 min, haemoglobin <90 g/L or haematocrit <35, broken or scarred skin overlying study site, previous allergic reaction to aquagel (or topical creams, preservatives in creams) and known pregnancy.

In the event of significant atheromatous plaque being detected in those with CHD, the findings were discussed in the clinic by SR, whilst in the case of volunteers (three individuals) the general practitioner was informed of the findings via letter with advice on assessing CVD risk factors, including lipoprotein(a), an independent risk marker associated with CVD and CVD risk lowering treatment. None of the scanned patients withdrew from the study or suffered adverse effects during the scanning process. There were no complaints of inconvenience in attending the given appointment. No data could be obtained in one patient due to interference in the cervical region (left and right). The patient was informed of this and scanning was aborted.

Ethics committee approval was obtained from the Health Research Authority (West Midlands – Solihull
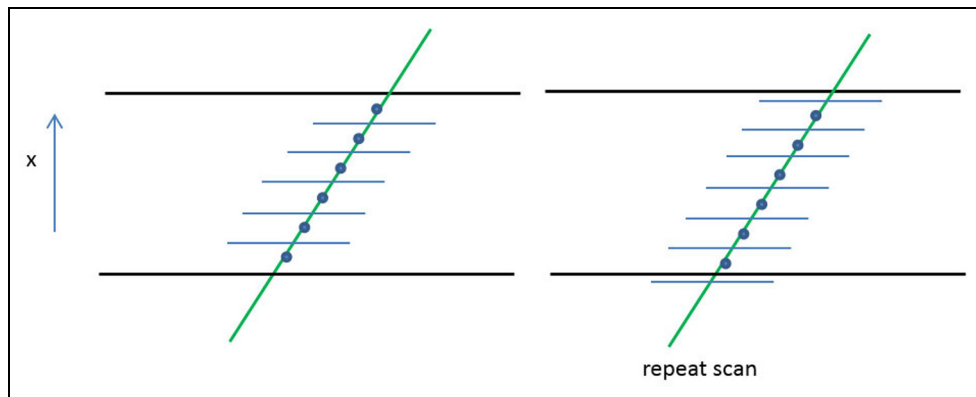
Figure 3. Repeat off-set scan test were conducted by translating the measurement points by half of the interrogation window size.

Research Ethics Committee; 15/WM/0164, IRAS project ID 164622). The Heart of England NHS Foundation Trust (now University Hospitals Birmingham NHS Foundation Trust) acted as the sponsor (Study Number: VascUsValidation2014) while the study was conducted in accordance with the submitted protocols. As the study was primarily investigating methodology we were precluded from obtaining demographic data from controls.

Ultrasound assessment

All US measurements were conducted in accordance with the 'Joint Recommendations for Reporting Carotid Ultrasound Investigations in the United Kingdom'.[27] The Mindray M9 US scanner was selected in view of availability and portability, its specifications can be found on the web.[28] A Linear 14–4 MHz transducer with a frequency of 9 MHz (with Harmonics on) was used with a sample volume of 0.5 mm. An angle of 60° was used when measuring flow so that results were as accurate as possible. The depth on screen (only accurate to 0.1 cm) was used to check each image to ensure correct positioning when sampling in B mode (Acoustic Power was 96.6%, depth 4 cm, gain 28, frame rate 46, dynamic range 110, iClear 4, iBeam1). The scanning was carried out by a vascular ultrasonographer working for both, Mindray and the University of Birmingham NHS Foundation Trust.

Due to easy accessibility the Common Carotid Artery (CCA) was chosen as the site best suited for this phase of the study. In view of anatomical variation of the CCA and its bifurcation into the external carotid artery (ECA) and internal carotid artery (ICA) it was necessary to establish a standardised scanning protocol. Figure 2 provides a diagrammatic illustration of the data collection site.

US velocity data was collected in position 1 as seen in Figure 2. Initially position 2 was identified, being 2.5 cm away from junction where the CCA bifurcates into the ICA and ECA, thus ensuring that the outlet boundary to be applied in the CFD model is sufficiently far away from the junction (position 2) to cause any negative impact on the accuracy of the computational model. The inlet for the CFD model was taken to be 3 cm upstream (position 1). The scanning angle α, was fixed to 60° for all measurements.

A number of pre-tests were conducted to establish an appropriately resolved cross-sectional velocity profile including varying the size of the interrogation window and the number of fixed increment steps. To improve the resolution also an off-set scan repetition was conducted as illustrated in Figure 3. Starting from an initial 2 mm interrogation window (pre-set), the increment steps were repeatedly halved to optimise the velocity profile resolution. The optimal scanning increments were found to be 0.5 mm in the central region reducing to 0.2 mm in the near-wall region. The influence of the scanning direction was found to be negligible.

CFD simulations

The mean peak systolic (PS) velocity profile was extracted from the US scans to reconstruct the inlet velocity profile for the CFD simulations (Figure 4(a)). Due to the scanning resolution decreasing near the wall the profile close to the wall was constructed by estimating the boundary layer thickness based on the Womersley number which was calculated from the heart rate. From the scan data it was estimated whether a near wall measurement fell in the boundary region or not. Depending on this estimate either two or three points were added allowing to complete the profile to the wall linearly (Figure 4(b)). Subsequently the data was smoothed in order to obtain a representative profile as the original raw data is affected by some noise (red crosses in Figure 4(b)). This was anticipated to allow reasonably accurate predictions of WSS even close to the inlet boundary.
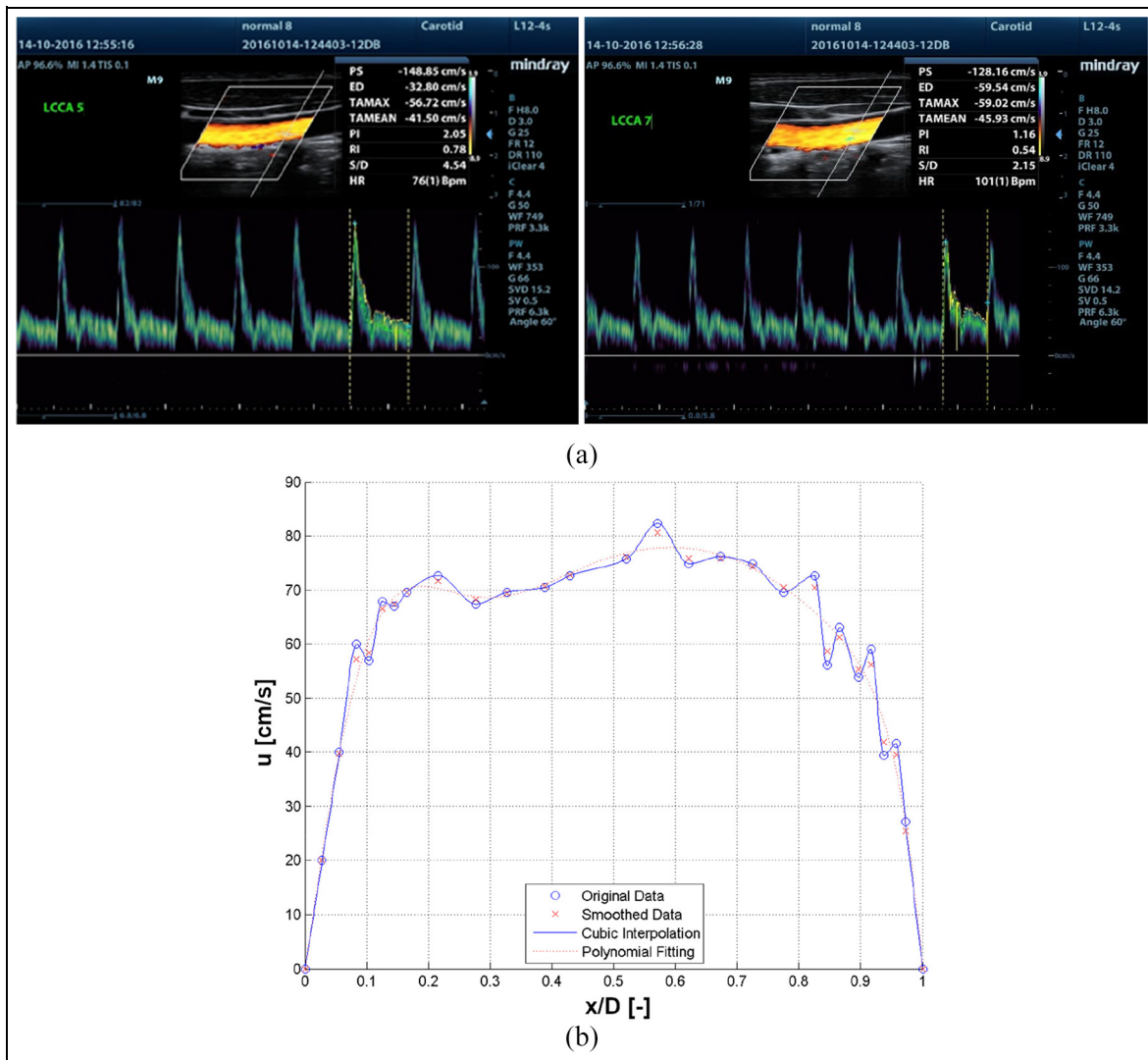
Figure 4. Velocity profile reconstruction: (a) sample US velocity readings and (b) sample velocity profile reconstruction (x-axis is the normalized local coordinate across the diameter, y-axis is the velocity in the x direction).

The scale dimensions were obtained from the 2D US scan images and shown in Figure 5(a). Using a free-ware digitising software (WebPlotDigitizer) the wall profile for each subject was extracted point wise using a fine spatial discretisation and then processed with a Matlab script to smooth, resample, rotate and cut to generate a suitable, high quality 2D geometry to be used in the CFD simulation which was performed using Ansys Fluent. An example of this reconstruction is presented in Figure 5(b). It is also noteworthy that the Matlab script identified the centre line of the individual CCA segment.

The above described geometry manipulation allowed for the application of horizontal inlet boundary conditions as well as avoiding any possible interference from the bifurcation beyond the outlet. The geometry was meshed including a proper size bias in the vertical direction to enhance grid resolution. This was achieved by ensuring approximately squared cells in the central region of the domain and thinner cells in the near-wall region, provided that a maximum cell aspect ratio was respected. The example in Figure 6 demonstrates the resulting grid distribution based on approximately 2000 mesh cells while the results were extracted from mesh sizes of approximately 45,000 cells. Estimating the velocity, u, and the friction factor, f, a maximum $y+$ value was also imposed along the wall. This was carried out, despite the flow being in the laminar region to ensure that a fine grid resolution at the wall was achieved enabling obtainment of accurate WSS values. The result of a conducted mesh independence test based on average cell size versus average WSS values obtained is reported in Figure 7. The average cell size chosen for the simulations is identified by the vertical black line in the image. Zero cell size value is predicted using the Richardson extrapolation method.[29] The US
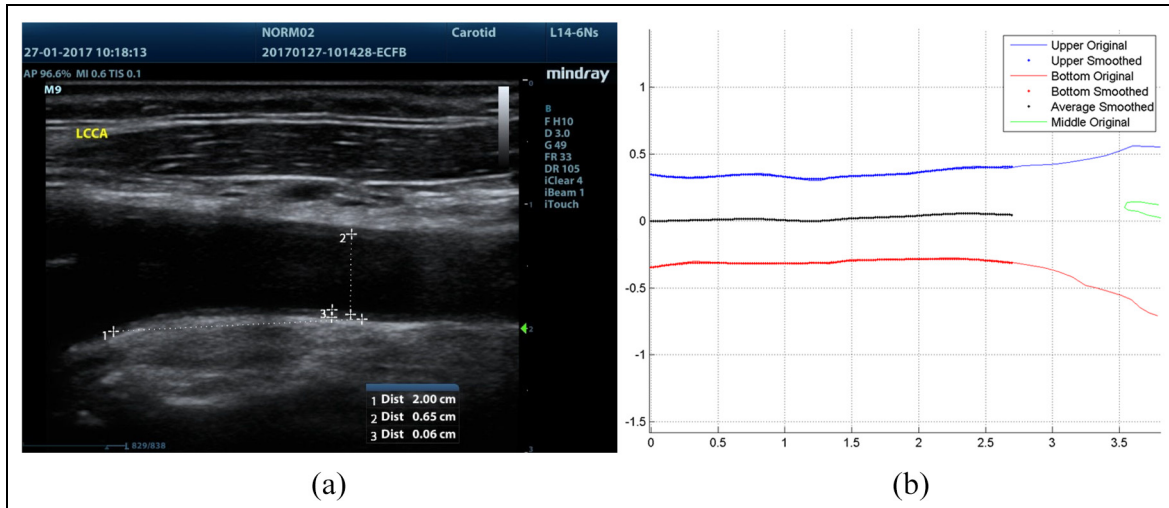
Figure 5. Geometry identification: (a) scale determination and (b) geometric reconstruction and midline determination; the image in (b) is a mirror image to (a).
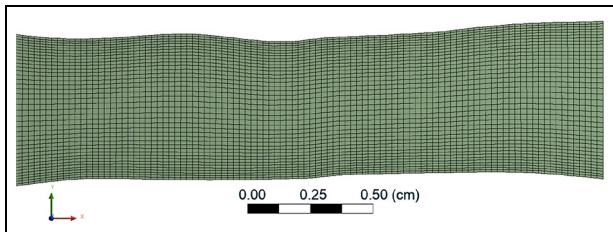

Figure 6. Resulting mesh distribution indicatively demonstrated for a mesh size of 2000 cells.

determined velocity profile was imposed as inlet boundary condition, whereas wall BCs were set at the walls, and a reference pressure was set at the outlet boundary. The fluid flow was treated as 2D, laminar and steady state. To model the non-Newtonian behaviour of blood the Carreau model was applied for the blood viscosity. Dynamic viscosity is modelled as dependent upon shear rate, and independent from temperature as follows

$$\mu = \mu_\infty + (\mu_0 - \mu_\infty)\left(1 + \dot{\gamma}^2\lambda^2\right)^{\frac{n-1}{2}} \quad (1)$$

where μ is the dynamic viscosity and $\dot{\gamma}$ the shear rate. Infinite shear viscosity was set to $\mu_\infty = 3.5\text{e}{-}3\,\text{kg/ms}$, zero shear viscosity to $\mu_0 = 5.6\text{e}{-}2\,\text{kg/ms}$, relaxation time to $\lambda = 3.313\,\text{s}$ and power law index $n = 0.3568$ according to Siebert and Fodor.[30] Blood density was set to $1050\,\text{kg/m}^3$. All flow variables were set to second order of accuracy and the convergence level reached by the simulations was such that the maximum residuals were $< 10^{-8}$. The CFD code used for the fluid flow simulations was Ansys-Fluent.

The numerical model described above was validated against analytical solutions for the laminar steady flow of a Carreau fluid in 2D parallel-plates channel geometry from the literature.[31] There the volumetric flow rate
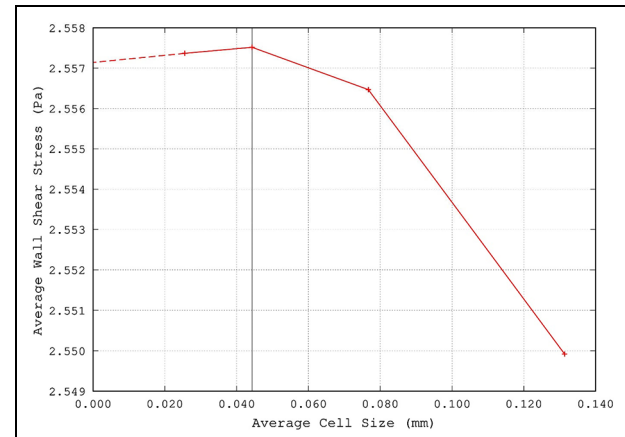

Figure 7. Mesh independence test shown for average WSS as a function of mesh size (black line indicates the average cell size used in this study).

$\dot{V}$ is expressed as function of the channel geometry (width W and height H), wall shear stress τ_w, and an integral involving shear rate and shear stress in the channel as

$$\dot{V} = \frac{WH^2}{2\tau_w^2} \int_0^{\tau_w} \dot{\gamma}\tau\,\mathrm{d}\tau \quad (2)$$

The integral in equation (1) is then analytically solved and expressed in terms of sums of hypergeometric functions involving the fluid rheological properties. For a given channel geometry and volumetric flow rate, by evaluating the integral

$$I = \int_0^{\tau_W} \gamma\tau^2 d\tau \quad (3)$$

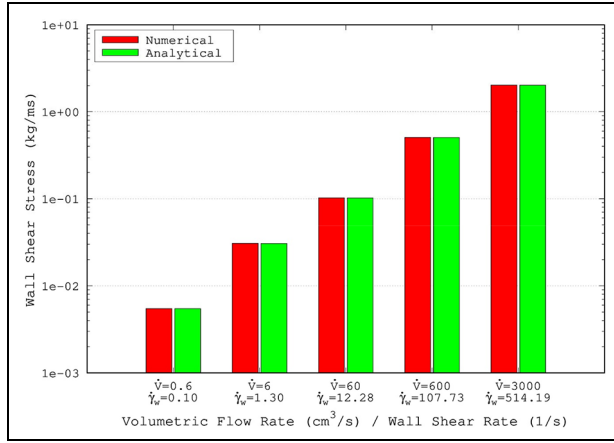as from[31] the wall shear stress can thus be analytically derived as

Figure 8. Validation tests for Carreau fluid for laminar flow in a 2D parallel-plates channel.

For validation purposes a series of CFD analyses were carried out for the steady laminar flow in a 2D parallel-plates channel. The chosen channel had comparable size to the simulated arteries (height H = 6 mm, length L = 3 cm) and was meshed following the same strategy. The fluid properties were the same and a periodic boundary condition was used for the inlet/outlet sections in order to model a fully-developed flow. Simulations were run for different volumetric flow rates (namely, 0.6, 6, 60, 600 and 3000 cm^3/s) in order to span shear rate values at the wall approximately in the range [0.1, 500]. WWS values were then extracted from the simulations and compared to the ones predicted analytically. Results of the validation are shown in Figure 8 where the maximum discrepancy between the numerical and the analytical model is found to be < 0.5%.

$$\tau_w = \sqrt{\frac{WH^2I}{2\dot{V}}} \qquad (4)$$

Statistical analysis

The variables measured included mean peak systolic (PS) velocity, velocity gradient and profiles and values derived such as WSS assessed by US measurements at
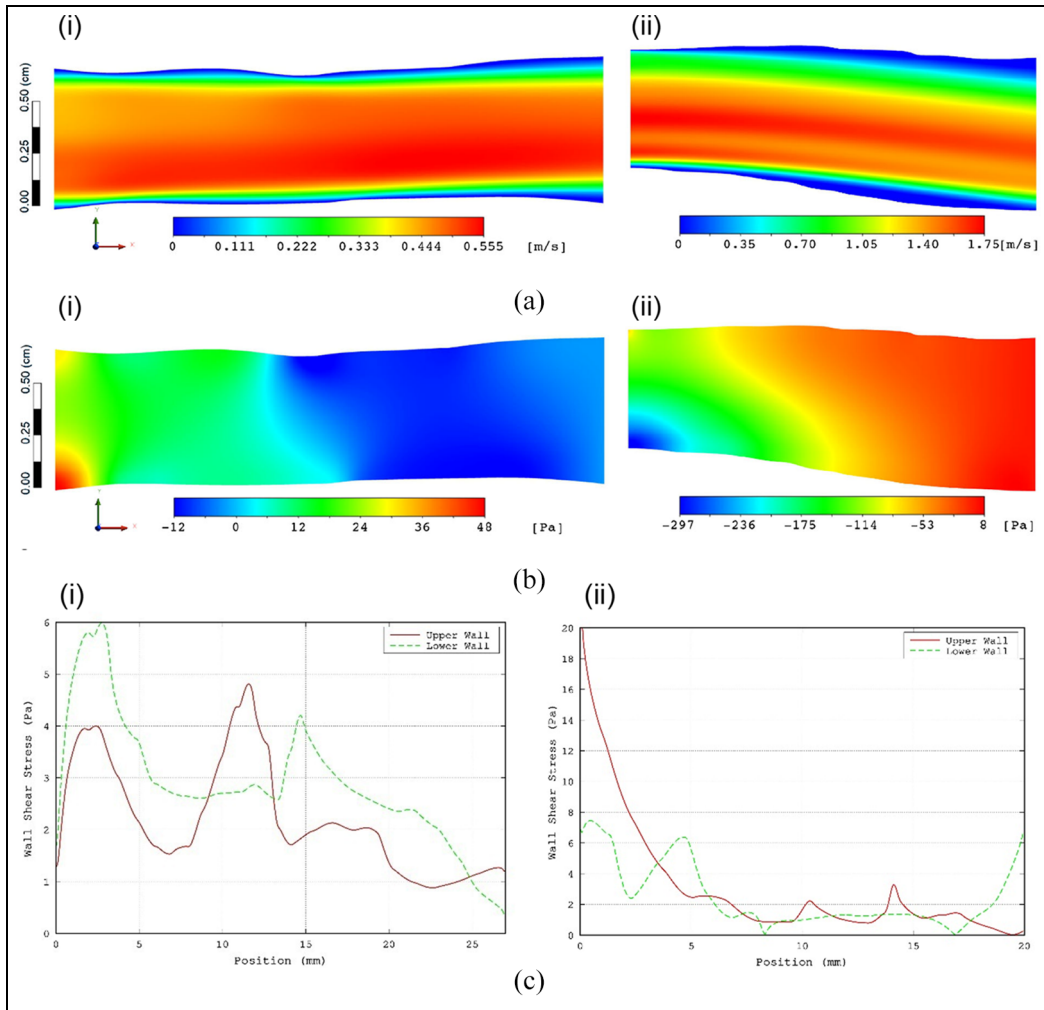

Figure 9. Typical results obtained from the CFD simulation: (a) iso-velocity-contours, (b) iso-pressure contours, and (c) WSS along the walls. (i and ii) refer to a healthy and a CVD subject, respectively.

peak systole in the common carotid artery (CCA) and shown in Table 1. Initially *t*-tests were carried out to establish if any of these measured/derived parameters (independent variables) differed between individuals with established CHD and those without CHD symptoms (dependent variable). The number of patients and the preliminary nature of this pilot study did not allow multiple regression analysis where confounders could be adjusted for. Factors that were significantly different between the patient groups were further investigated (dependent variables) with linear regression (in the event of continuous distribution) or logistic regression (in the event of a dichotomous outcome) carried out to establish other associated factors (independent variables).

Results

Numerical results

Figure 9 shows typical results as obtained from two exemplary CFD simulation cases (one healthy and one CVD) such as iso-contours of velocity (Figure 9(a)) and pressure (Figure 9(b)) as well as the corresponding wall shear stress (WSS) distributions along the walls (Figure 9(c)). As would be anticipated for steady flow the flow distribution is strongly dependent on the imposed inlet velocity profile in the central, non-boundary regions of the simulation domain. In areas where the CCA widens due to the slightly irregular nature of the vessel wall the near wall regions show an extended region of low velocity flow due to the jet effect of the core flow. This results in different velocity gradients along the wall causing significant variation of the WSS as can be seen in Figure 9(c). Following the completion of all simulations, a thorough data analysis was conducted which included skewness and kurtosis of velocity profiles amongst other calculations of as well as calculation of the percentage areas where the WSS was found to be below certain threshold values (WSS < 1, WSS < 2 and WSS < 3 Pa).

Comparison of measured and derived parameters: Between group evaluation

Table 1 shows the measured and derived variables gathered for each scanned individual using the methodology described in the previous section. We looked for differences in US data and CFD outputs between two groups of patients (with established CHD vs no evidence of CHD) via unpaired *t*-tests (Table 2). Associations between significant US factor(s) relating to the CFD outputs (independent variables) and other measured/derived factors (dependent variables) were determined by linear regression analyses.

Table 2 shows that mean PS velocity was associated with CHD; individuals without CHD: mean (SD) = 62.8 (16.1) cm/s, with CHD: mean (SD) = 53.6 (17.3) cm/s, $p = 0.042$. None of the other measured or derived factors was statistically different between the 2

cohorts. Linear regression analyses in Table 3 showed that PS velocity was associated with the following CFD outputs: average pressure drop in the carotid bulb ($p < 0.001$), area of WSS in the location of the bulb less than 1 Pa ($p = 0.016$), area of WSS in the location of the bulb less than 2 Pa ($p = 0.006$), area of WSS in the location of the bulb less than 3 Pa ($p = 0.001$) and area of WSS upstream of the bulb less than 3 Pa ($p = 0.017$).

Discussion

The aim of the study was to evaluate the necessary dataset enabling ultrasound based measured and derived flow data to be used clinically. We then compared these parameters in individuals with established CHD and those not experiencing symptoms of CVD. Our results in conjunction with other studies suggest that PS velocity may be an area of interest. Even with a small number of subjects a significant difference was observed between the 27 patients with diagnosed CHD and the 30 individuals without CVD symptoms. It was also interesting that the PS velocity was associated with many other factors that we measured/derived that were of interest in atherogenesis.

Previous research has hinted that PS velocity, a robust and easily obtainable non-invasive measure in various vascular beds may be possibly a suitable identifier associated with atherogenesis. Chuang et al.[32] obtained baseline quantitative CCA US data from the Cardiovascular Diseases Risk Factor Two-Township Study in 3146 Taiwanese adults and studied ischaemic heart disease ($n = 220$) and strokes ($n = 247$) after a median follow-up of 12.8 years. PS velocity (< 65 cm/s vs ≥ 80 cm/s) was associated with CVD (Hazard ratio: 3.23, 95% confidence intervals: 2.51–4.15, $p < 0.0001$). It must be stated that end diastolic pressure (< 15 cm/s vs ≥ 20 cm/s) was even better at identifying CVD (Hazard ratio: 4.54, 95% confidence intervals: 3.51–5.85, $p < 0.0001$). Chung et al.[33] in the I-Lan Longitudinal Aging Study found that low PS and end diastolic velocities were associated with cognitive dysfunction as assessed by mini-Mental State Examination and neuropsychological tests in 1684 Taiwanese subjects without cognitive impairment at baseline. Zhang et al.[34] found in their patient study that carotid artery plaque score (CAPS), combined with the PS velocity of the right internal carotid artery has a greater predictive value for CHD than CAPS alone.

Westholm et al.[35] estimated the prognostic function of PS velocity in the basal segments of the left ventricle obtained from tissue Doppler imaging in 227 acute coronary syndrome patients. They found that a composite outcome of death, re-admission related to acute coronary syndrome and heart failure was associated independently with lower PS velocity. Further, it appeared that PS velocity was more predictive of the monitored outcome (estimated via area under the receiver operated

Table 1. Measured and derived variables from the US scan on each individual.

Variable	Derivation	Unit	Mean ± SD
L-CCA lumen	Measured from scan	cm	0.67 ± 0.11
Scan distance	Measured from scan	cm	2.13 ± 0.33
Avg heart rate	Measured from scan	bpm	66.47 ± 10.54
Max heart rate	Measured from scan	bpm	72.77 ± 11.87
Min heart rate	Measured from scan	bpm	60.27 ± 9.67
Max ± Min heart rate ratio	Derived from scan	–	1.21 ± 0.13
Heart rate Std Dev	Derived from scan	bpm	3.77 ± 2.44
Avg Womersley number	Derived from scan	–	4.87 ± 0.80
Expected boundary layer thickness	Derived from scan	mm	0.70 ± 0.05
Average PS velocity	Derived from scan	cm/s	59.16 ± 16.42
PS mass flow rate	Derived from scan	g/s	22.56 ± 8.93
Avg PS Reynolds number	Derived from scan	–	1199.00 ± 371.10
Avg velocity	Derived from scan	cm/s	0.49 ± 0.02
Velocity std dev	Derived from scan	cm/s	0.25 ± 0.01
Velocity profile skewness	Derived from scan	–	0.04 ± 0.09
Velocity profile kurtosis	Derived from scan	–	1.94 ± 0.06
L-CCA lumen	CFD model	mm	6.72 ± 1.03
Inlet section length	CFD model (bulb)	mm	6.72 ± 1.03
Outlet section length	CFD model (bulb)	mm	7.28 ± 1.51
Upper wall length	CFD model (bulb)	mm	26.18 ± 3.77
Lower wall length	CFD model (bulb)	mm	26.30 ± 3.54
Avg dynamic viscosity at inlet section	CFD model (bulb)	cP	5.37 ± 0.70
Avg dynamic viscosity at outlet section	CFD model (bulb)	cP	5.20 ± 0.60
Avg dynamic viscosity at upper wall	CFD model (bulb)	cP	4.66 ± 0.90
Avg dynamic viscosity at lower wall	CFD model (bulb)	cP	4.40 ± 0.94
Avg static pressure at inlet section	CFD model (bulb)	Pa	55.43 ± 122.39
Avg static pressure at outlet section	CFD model (bulb)	Pa	-0.01 ± 0.02
Relative Pressure drop	CFD model (bulb)	Pa/m	2214.92 ± 5046.03
Avg total pressure at inlet section	CFD model (bulb)	Pa	352.98 ± 211.77
Avg total pressure at outlet section	CFD model (bulb)	Pa	300.79 ± 193.40
Relative total pressure drop	CFD model (bulb)	Pa/m	2055.91 ± 1840.34
Avg WSS at upper wall	CFD model (bulb)	Pa	2.95 ± 1.78
Avg WSS at lower wall	CFD model (bulb)	Pa	3.47 ± 2.04
Inlet section length	CFD model (upstream)	mm	6.54 ± 1.16
Outlet section length	CFD model (upstream)	mm	7.13 ± 1.16
Upper wall length	CFD model (upstream)	mm	21.99 ± 4.78
Lower wall length	CFD model (upstream)	mm	22.16 ± 4.73
Avg dynamic viscosity at inlet section	CFD model (upstream)	cP	5.27 ± 0.69
Avg dynamic viscosity at outlet section	CFD model (upstream)	cP	5.28 ± 0.73
Avg dynamic viscosity at upper wall	CFD model (upstream)	cP	4.07 ± 0.45
Avg dynamic viscosity at lower wall	CFD model (upstream)	cP	4.07 ± 0.60
Avg static pressure at inlet section	CFD model (upstream)	Pa	7.74 ± 57.82
Avg static pressure at outlet section	CFD model (upstream)	Pa	0.00 ± 0.00
Relative Pressure drop	CFD model (upstream)	Pa/m	266.80 ± 2775.70
Avg total pressure at inlet section	CFD model (upstream)	Pa	335.24 ± 178.82
Avg total pressure at outlet section	CFD model (upstream)	Pa	286.64 ± 156.16
Relative total pressure drop	CFD model (upstream)	Pa/m	2325.03 ± 1641.38
Avg WSS at upper wall	CFD model (upstream)	Pa	3.39 ± 2.21
Avg WSS at lower wall	CFD model (upstream)	Pa	3.16 ± 1.13
Avg WSS	CFD model (bulb)	Pa	3.18 ± 1.76
WSS variance	CFD model (bulb)	Pa^2	7.55 ± 13.82
WSS std dev	CFD model (bulb)	Pa	2.26 ± 1.57
WSS 3rd order moment	CFD model (bulb)	Pa^3	30.99 ± 83.86
WSS skewness	CFD model (bulb)	–	0.75 ± 0.53
WSS 4th order moment	CFD model (bulb)	Pa^4	648.17 ± 2369.66
WSS kurtosis	CFD model (bulb)	–	3.25 ± 1.25
WSS area < 1 Pa	CFD model (bulb)	%	26.17 ± 17.93
WSS area < 2 Pa	CFD model (bulb)	%	41.55 ± 22.07
WSS area < 3 Pa	CFD model (bulb)	%	57.98 ± 24.31
Avg WSS	CFD model (upstream)	Pa	3.23 ± 1.20
WSS variance	CFD model (upstream)	Pa^2	4.61 ± 7.89
WSS std dev	CFD model (upstream)	Pa	1.83 ± 1.13
WSS 3rd order moment	CFD model (upstream)	Pa^3	18.97 ± 51.40
WSS skewness	CFD model (upstream)	–	0.91 ± 0.76

(continued)

Table 1. Continued

Variable	Derivation	Unit	Mean $\pm$ SD
WSS 4th order moment	CFD model (upstream)	Pa^4	272.24 $\pm$ 1152.84
WSS kurtosis	CFD model (upstream)	–	4.09 $\pm$ 2.05
WSS area < 1 Pa	CFD model (upstream)	%	13.17 $\pm$ 15.02
WSS area < 2 Pa	CFD model (upstream)	%	31.93 $\pm$ 23.81
WSS area < 3 Pa	CFD model (upstream)	%	55.49 $\pm$ 25.48
Min upstream artery diameter ($\varnothing$)	Derived from scan	cm	0.63 $\pm$ 0.10
Max bulb artery $\varnothing$ (without bifurcation)	Derived from scan	cm	0.86 $\pm$ 0.17
Max bulb artery $\varnothing$ (with bifurcation)	Derived from scan	cm	0.83 $\pm$ 0.14
Max $\pm$ Min artery $\varnothing$ ratio (without bifurcation)	Derived from scan	–	1.38 $\pm$ 0.26
Max $\pm$ Min artery $\varnothing$ ratio (with bifurcation)	Derived from scan	–	1.34 $\pm$ 0.21

Table 2. Unpaired t-tests comparing volunteers ($n = 30$) with patients (coronary heart disease). Only velocity was significantly different between the two groups.

Variable	Controls (No CVD), $n = 30$ mean (SD)	CHD, $n = 27$ mean (SD)	p
Avg PS velocity (cm/s)	62.8 (16.1)	53.6 (17.3)	0.042
Avg static pressure (upstream) drop (Pa/m)	2950.3 (6473.3)	1317 (2417.8)	0.22
Avg total pressure (upstream) drop (Pa/m)	2208.3 (1761.1)	1811.9 (1942.4)	0.42
CFD WSS distribution (bulb) avg Pa	3.5 (2.1)	5.0 (11.3)	0.46
CFD WSS distribution (bulb) std dev Pa	3.6 (2.0)	4.2 (11.8)	0.48
CFD WSS distribution (bulb) area < 1 Pa	24.5 (18.3)	29.5 (18.9)	0.32
CFD WSS distribution (bulb) area < 2 Pa	41.1 (21.2)	43.1 (23.6)	0.74
CFD WSS distribution (bulb) area < 3 Pa	57.5 (23.2)	59.0 (25.6)	0.82
CFD WSS distribution (upstream) avg Pa	3.2 (1.3)	5.7 (13.3)	0.34
CFD WSS distribution (upstream) std dev Pa	2.1 (1.4)	4.3 (14.0)	0.39
CFD WSS distribution (upstream) area < 1 Pa	15.2 (15.4)	13.3 (19.3)	0.69
CFD WSS distribution (upstream) area < 2 Pa	32.2 (22.9)	33.5 (26.5)	0.84
CFD WSS distribution (upstream) area < 3 Pa	55.6 (24.7)	56.4 (26.8)	0.91

curve) and less dependent on image quality than other measures obtained from an echocardiography such as ejection fraction, wall motion scoring and 2D strain.

Erectile dysfunction appears to be a powerful predictor of CVD, CHD and all-cause mortality.[36,37] Thus, it is worth studying markers of atherogenesis in men included within this high CVD risk clinical presentation phenotype. Vicari et al.[38] measured penile PS velocity in 65 consecutive men suffering from erectile dysfunction and found that lower PS velocity was associated with generalised atherosclerosis. Previously El-Sakka and Morsy[39] had suggested that CHD was associated with penile lower PS velocity. They studied 303 men with erectile dysfunction and found that 31.4% had ischaemic heart disease which was associated with low PS velocity (but not end diastolic velocity) in the cavernosal arteries. Further, greater severity of ischaemic heart disease was related to lower PS velocity values and they suggested penile US as a screening tool in men with erectile dysfunction. Gupta et al.[40] reviewed the role of penile US as a predictor of CVD in view of traditional CVD risk factors such as diabetes, obesity, diet and physical activity only identifying half of high risk individuals. They carried out penile Doppler US in 49 men with erectile dysfunction prior to stress echocardiography which showed abnormalities in 20% of the men. PS velocity < 30 cm/s was significantly associated with abnormalities.

The association between PS velocity and atherogenesis must not be mistaken for causality. It is possible that PS velocity is associated with many factors such as for example endothelial dysfunction or arterial stiffness that may contribute to atheroma formation and hence may be a superior predictor than each of these factors considered separately. It could be that PS velocity is a surrogate for many factors, hence it possesses greater predictive ability. It is possible that WSS may be one such causative factor (although our data does not suggest this –Table 2). Low WSS (WSS < 1, < 2 and < 3 Pa) as expected was inversely correlated with PS velocity in our analysis (Table 3). A prospective study of the association between WSS and atherogenesis will require a significantly larger cohort and include many other confounders that may either be associated with WSS and/or the pathogenesis of atheroma. Such analyses may point to the exact role PS velocity plays in atherogenesis, either a mediator or a surrogate marker.

The above data suggests a potential predictive role for PS velocity in various vascular beds. However, it is essential to standardise the data collection and collect

Table 3. Separate linear regression models studying the association between the various outcome variables and mean PS velocity. All the models included the two groups of the cohort factorised (volunteers = reference, CHD patients compared to reference) as CHD was associated with velocity. CHD was not associated with the selected outcomes in any of the analyses (data not shown).

Outcome (dependent variable)	Average PS velocity (cm/s) c (95% CI)	p
Mean static pressure (bulb) drop Pa/m	43.0 (−37.8 to 123.7)	0.29
Mean total pressure (bulb) drop Pa/m	58.5 (32.8 to 84.3)	< 0.001
CFD WSS distribution (bulb) avg Pa	−0.08 (−0.2 to 0.04)	0.19
CFD WSS distribution (bulb) std dev Pa	−0.1 (−0.2 to 0.03)	0.14
CFD WSS distribution (bulb) area < 1 Pa	−0.4 (−0.6 to −0.1)	0.016
CFD WSS distribution (bulb) area < 2 Pa	−0.5 (−0.8 to −0.1)	0.006
CFD WSS distribution (bulb) area < 3 Pa	−0.7 (−1.0 to −0.3)	0.001
CFD WSS distribution (upstream) avg Pa	−0.1 (−0.3 to 0.02)	0.083
CFD WSS distribution (upstream) std dev Pa	−0.1 (−0.3 to 0.03)	0.1
CFD WSS distribution (upstream) area < 1 Pa	−0.06 (−0.3 to 0.2)	0.68
CFD WSS distribution (upstream) area < 2 Pa	−0.2 (−0.6 to 0.2)	0.35
CFD WSS distribution (upstream) area < 3 Pa	−0.5 (−0.9 to −0.09)	0.017

robust data with optimal precision and accuracy in differing patient groups (e.g. gender, height, weight/waist circumference, ethnicity, diabetes/metabolic syndrome and underlying risk factors), arteries varying in diameter and equipment differing in resolution, practicality etc. Our data and dataset obtained is strictly applicable to the Mindray M9 portable US. It is essential that all US equipment manufacturers are aware of the potential use of PS velocity as a screening tool and carry out optimisation enabling accurate and precise readings that could be clinically useful. Interestingly Song et al.[41] described a new wireless carotid neckband Doppler system containing US sensors which measured PS velocity comparable to a conventional US machine. This system could potentially add to the type of studies currently designed allowing flow measurements over a longer period of time.

Study strengths and limitations

Although the cohort was small, the study has provided some interesting findings. We used a portable ultrasound machine and replicated the association between PS velocity and CHD, which will be useful for future studies regarding convenience. Portable equipment such as ours would allow a wider patient catchment in future studies. Following validation of our findings, PS velocity via portable US equipment could be used as an identifier and possibly also as a predictor, not just in a central location, but also potentially in primary care. The fact that previously reported associations between PS velocity and CHD in the carotid artery and other vascular beds was confirmed in such a small patient group using portable equipment with relatively low resolution suggests an important role for PS velocity as a predictor of atherogenesis. However, the modest cohort precluded us from recording demographic variability and subsequent stratifying the patient group (e.g. age, gender etc.) and studying factors associated with CHD. Further, it also prevented us from using combinations of factors as independent variables. Many other factors of interest were associated with PS velocity and these associations must be studied in detail in a larger cohort with patients stratified by treatment(s), age, gender, vascular pathology etc. It is apparent that the current US technology lacks the resolution for estimating L-CCA velocity profile. However, newer technology is entering the market that promises to provide direct measurement of the velocity profile. Lastly it would have been interesting to study the association between vascular flow properties and atherogenesis in a longitudinal study.

Conclusion

Ours was a pilot study with two end points; assessing the feasibility of using a portable US machine to study blood flow factors in a routine clinical setting and investigating associations between flow measurements and CHD. The data from the scans suggest that low-cost US measurement could principally be a suitable and capable tool but a greater resolution is required for assessment of flow for both, ease and accuracy. Radio frequency data output which is available in more sophisticated equipment is desirable due to the advantages of ease of data processing. It is interesting that mean PS velocity differed between the patient groups. We would in the future like to further investigate the mean PS velocity as a prognostic marker in blood vessels varying in diameter (including adjustment for medication and severity of atheroma in patients using angiogram results etc) for atherosclerosis. Thus, PS velocity which is a robust easily measured factor may be important as a non-invasive real time marker of atherogenesis that could have major clinical use.

Declaration of conflicting interests

Funding

ORCID iDs

Carola S König (iD) https://orcid.org/0000-0002-9289-3154
Mark Atherton (iD) https://orcid.org/0000-0002-3293-4241
Marco Cavazzuti (iD) https://orcid.org/0000-0001-6289-9507

References

1. BHF. Cardiovascular Disease Statistics, 2018, https://www.bhf.org.uk/what-we-do/our-research/heart-statistics/heart-statistics-publications/cardiovascular-disease-statistics-2018 (accessed 5 January 2020).
2. Ramachandran S, Bhartia M and König CS. The lipid hypothesis: from resins to proprotein convertase subtilisin/kexin type-9 inhibitors. In: *Frontiers in cardiovascular drug discovery*, vol. 5. Bentham Books, 2019, pp.48–81.
3. NICE. Cardiovascular disease: risk assessment and reduction, including lipid modification, https://www.nice.org.uk/guidance/cg181 (accessed 5 January 2020).
4. British Cardiac Society, British Hypertension Society, Diabetes UK, et al. JBS 2: Joint British Societies' guidelines on prevention of cardiovascular disease in clinical practice. *Heart* 2005; 91(Suppl. 5): v1–52.
5. JBS3 Board. Joint British Societies' consensus recommendations for the prevention of cardiovascular disease (JBS3). *Heart* 2014; 100(Suppl. 2): ii1–ii67.
6. Shipman KE, Strange RC and Ramachandran S. Use of fibrates in the metabolic syndrome: a review. *World J Diabetes* 2016; 7: 74–88.
7. Ramachandran S, Bhartia M, Jones A, et al. Use of fibrates in the metabolic syndrome and diabetes: practical tips. In: *RSSDI diabetes update*. New Delhi, India: Jaypee Brothers Medical Publishers Ltd, 2018, pp.356–361.
8. Gimbrone MA and Garcia-Cardena G. Endothelial cell dysfunction and the pathobiology of atherosclerosis. *Circ Res* 2016; 118: 620–636.
9. Chhabra N. Endothelial dysfunction – a predictor of atherosclerosis. *Internet J Med Update* 2009; 4: 33–41.
10. Chiu J-J and Chien S. Effects of disturbed flow on vascular endothelium: pathophysiological basis and clinical perspectives. *Physiol Rev* 2011; 91: 327–387.
11. Halcox JPJ, Donald AE, Ellins E, et al. Endothelial function predicts progression of carotid intima-media thickness. *Circulation* 2009; 119:1005–1012.
12. Yamaoka-Tojo M. Endothelial function for cardiovascular disease prevention and management. *Int J Clin Cardiol* 2017; 4(3): 1–11.
13. Baratchi S, Khoshmanesh K, Woodman OL, et al. Molecular sensors of blood flow in endothelial cells. *Trends Mol Med* 2017; 23: 850–868.
14. Peiffer V, Sherwin SJ and Weinberg PD. Does low and oscillatory wall shear stress correlate spatially with early atherosclerosis? A systematic review. *Cardiovasc Res* 2013; 99: 242–250.
15. Zhou J, Li YS and Chien S. Shear stress-initiated signaling and its regulation of endothelial function. *Arterioscler Thromb Vasc Biol* 2014; 34: 2191–2198.
16. Nayak A, König CS, Kishore U, et al. Regulation of endothelial activation and vascular inflammation by shear stress. In: *Micro and nano flow systems for bioanalysis*. New York, NY: Springer, 2013, pp.77–86.
17. Warboys CM, Amini N, de Luca A, et al. The role of blood flow in determining the sites of atherosclerotic plaques. *F1000 Med Rep* 2011; 3: 5.
18. Malek AM, Alper SL and Izumo S. Hemodynamic shear stress and its role in atherosclerosis. *JAMA* 1999; 282: 2035–2042.
19. Gijsen F, Katagiri Y, Barlis P, et al. Expert recommendations on the assessment of wall shear stress in human coronary arteries: existing methodologies, technical considerations, and clinical applications. *Eur Heart J* 2019; 40: 3421–3433.
20. Cunningham KS and Gotlieb AI. The role of shear stress in the pathogenesis of atherosclerosis. *Lab Invest* 2005; 85: 9–23.
21. Zhang F, Lanning C, Mazzaro L, et al. In vitro and preliminary in vivo validation of echo particle image velocimetry in carotid vascular imaging. *Ultrasound Med Biol* 2011; 37(3): 450–464.
22. von Reutern G-M, Goertler M-W, Bornstein NM, et al. Grading carotid stenosis using ultrasonic methods. *Stroke* 2012; 43(3): 916–921.
23. Fraser KH, Poelma C, Zhou B, et al. Ultrasound imaging velocimetry with interleaved images for improved pulsatile arterial flow measurements: a new correction method, experimental and in vivo validation. *J R Soc Interface* 2017; 14(127): 20160761.
24. Gates PE, Gurung A, Mazzaro L, et al. Measurement of wall shear stress exerted by flowing blood in the human carotid artery: ultrasound Doppler velocimetry and echo particle image velocimetry. *Ultrasound Med Biol* 2018; 44(7): 1392–1401.
25. Faul F, Erdfelder E, Lang AG, et al. G*Power 3: a flexible statistical power analysis program for the social, behavioral, and biomedical sciences. *Behav Res Methods* 2007; 39: 175–191.
26. Gnasso A, Irace C, Carallo C, et al. In vivo association between low wall shear stress and plaque in subjects with asymmetrical carotid atherosclerosis. *Stroke* 1997; 28: 993–998.
27. Oates CP, Naylor AR, Hartshorne T, et al. Joint recommendations for Reporting Carotid Ultrasound Investigations in the United Kingdom. *Eur J Vasc Endovasc Surg* 2009; 37: 251–261.
28. Mindray. M9 Ultrasound System, http://www.mindray.com/en/product/M9_GI.html (accessed 5 January 2020).
29. Roache P. Quantification of uncertainty in computational fluid dynamics. *Ann Rev Fluid Mech* 1997; 29(1): 123–160.
30. Siebert MW and Fodor PS. Newtonian and non-Newtonian blood flow over a backward-facing step – a case study. In: *Proceedings of the Comsol conference*, Boston, Milan, Bangalore, 2009.
31. Sochi T. Analytical solutions for the flow of Carreau and Cross fluids in circular pipes and thin slits. *Rheologica Acta* 2015; 54(8): 745–756.

32. Chuang SY, Bai CH, Cheng HM, et al. Common carotid artery end-diastolic velocity is independently associated with future cardiovascular events. *Eur J Prev Cardiol* 2016; 23: 116–124.

33. Chung CP, Peng LN, Chou KH, et al. High circulatory phosphate level is associated with cerebral small-vessel diseases. *Transl Stroke Res* 2019; 10: 265–272.

34. Zhang H, Liu M, Ren T, et al. Associations between carotid artery plaque score, carotid hemodynamics and coronary heart disease. *Int J Environ Res Public Health* 2015; 12: 14275–14284

35. Westholm C, Johnson J, Sahlen A, et al. Peak systolic velocity using color-coded tissue Doppler imaging, a strong and independent predictor of outcome in acute coronary syndrome patients. *Cardiovasc Ultrasound* 2013; 11: 9.

36. Ma RC, So WY, Yang X, et al. Erectile dysfunction predicts coronary heart disease in type 2 diabetes. *J Am Coll Cardiol* 2008; 51: 2045–2050.

37. Dong JY, Zhang YH and Qin YQ. Erectile dysfunction and risk of cardiovascular disease meta-analysis of prospective cohort studies. *J Am Coll Cardiol* 2011; 58: 1378–1385.

38. Vicari E, Di Pino L, La Vignera S, et al. Peak systolic velocity in patients with arterial erectile dysfunction and peripheral arterial disease. *Int J Impot Res* 2006; 18:175–179.

39. El-Sakka AI and Morsy AM. Screening for ischemic heart disease in patients with erectile dysfunction: role of penile Doppler ultrasonography. *Urology* 2004 64: 346–350.

40. Gupta N, Herati A and Gilbert BR. Penile Doppler ultrasound predicting cardiovascular disease in men with erectile dysfunction. *Curr Urol Rep* 2015; 16: 16.

41. Song I, Yoon J, Kang J, et al. Design and implementation of a new wireless carotid neckband doppler system with wearable ultrasound sensors: preliminary results. *Appl Sci* 2019; 9: 2202.